Effect of Curing Conditions on the Fabrication of Zn-oxide Nanoparticles Dispersed in a Polyimide Film

HYUNG-GU ROH
GUN-HONG KIM
YOUNG-HO KIM[1]
Department of Materials Science & Engineering, College of Engineering, Hanyang University, Seoul 133-791, Korea

(Received 27 December 2005; accepted 8 March 2006)

Abstract: Zinc oxide nanoparticles were formed by reacting polyamic acid (PAA) with Zn during curing. In this paper, we investigated the effect of curing conditions on the zinc oxide nanoparticle formation. The polyimide (PI) precursors used in this study were biphenyltetracarboxylic dianhydride-*p*-phenylene diamine (BPDA-PDA) type and oxydiphthalic dianhydride 3-sulful dianhydride (ODPA-3SDA) type PAAs. Zn thin films were deposited on silicon substrates by DC magnetron sputter. PAA was then spin-coated onto Zn thin films and the PAA/metal films were cured at various conditions. The characterization using transmission electron microscope observation was carried out to investigate the size and distribution of zinc oxide particles. Zinc oxide nanoparticles were formed in the PI film regardless of the curing conditions. The size, distribution and density of zinc oxide particles were strongly dependent on the curing conditions..

Key Words: Nanoparticle, zinc oxide, polyimide, imidization, curing

1. INTRODUCTION

Polyimide (PI) is one of the most intriguing materials for microelectronic applications, because it has a low dielectric constant, outstanding thermal and chemical stability, desirable mechanical properties and high glass transition temperature [1–4]. Recently, dielectric materials containing nano-sized particles have received much attention from both the fundamental viewpoint and for applications in electrical and optical devices [5–8]. It is important to control the particle size, volume fraction of the particle phase, and also the spatial distribution of the particles in the film [5–9].

Various methods have been developed to fabricate the nanoparticles dispersed in polymer matrices [9–12], but these methods have the disadvantages of complex and

High Performance Polymers, **18:** 739–747, 2006 DOI:10.1177/0954008306068251

costly manufacturing processes [9] and furthermore, these processes were difficult to control [11].

We have previously developed a new method to fabricate nanoparticles in PI film by spin coating the PI precursor, polyamic acid (PAA), on thin metal films and imidization of PAA into PI [13–21]. The type of particles formed, the particle distribution, and the mechanism depend on the reactivity between PAA and thin metal films [15–21]. When the PAA was in contact with Zn or Cu thin films, the thin metal films reacted with PAA and were completely dissolved into PAA solution. During imidization of PAA into PI by thermal curing, oxide particles of the respective metal film were precipitated within the PI layer. The curing conditions had strong effects on the density and size of the nanoparticles formed in the PI matrix [20, 21]. The isothermal curing study of Cu_2O nanoparticle formation showed that very fine and uniform Cu_2O nanoparticles with high density were fabricated in the PI by controlling the curing time [21].

This research focuses on zinc oxide nanoparticle formation during isothermal curing and the effect of the curing atmosphere. After the PAA had reacted with the Zn films, the PAA Zn specimens were cured at 350°C in a nitrogen atmosphere or in vacuum for various times. In addition our study of zinc oxide nanoparticle formation was extended to optically transparent PI, oxydiphthalic dianhydride 3-sulful dianhydride (ODPA-3SDA) for optical applications.

2. EXPERIMENTAL PROCEDURE

The polyimide precursors used in this experiment were biphenyltetracarboxylic dianhydride-*p*-phenylene diamine (BPDA-PDA) type PAA (a commercial product, PI2610D; Dupont) dissolved in *N*-methyl-2-pyrrdidone (NMP) and ODPA-3SDA type PAA (synthesized in the lab.) in *N,N*-dimethylacetamide (DMAc). Figure 1 shows the chemical structures of BPDA-PDA type and ODPA-3SDA type PAA and imidization by thermal curing.

The 10-nm-thick Zn films were deposited onto Si or oxidized Si substrates by DC magnetron sputter. The PAA solutions were spin-coated onto Zn thin film substrates. Then the PAA Zn thin film stacks were soft-baked at 135°C for 30 min to evaporate the solvent. The ODPA-3SDA/metal stacks were cured at 250°C for 1 h in a nitrogen atmosphere and the BPDA-PDA/metal stacks were thermally cured at 350°C for from 1 to 4 h in a nitrogen atmosphere or in a vacuum. Transmission electron microscope (TEM) (JEM 2000, JEM 4010; JEOL) was used to characterize the nanoparticles formed in the PI films.

3. RESULTS

Figure 2 shows bright field TEM images of zinc oxide particles dispersed in BPDA-PDA type PI after curing at 350°C for 1, 2, and 4 h in a nitrogen atmosphere. Nano-sized particles were formed and randomly distributed in the PI film. When the specimen was cured

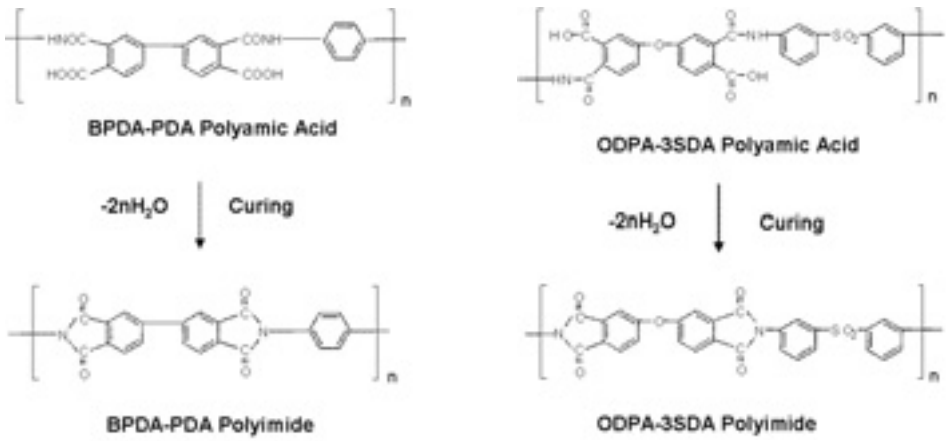

Figure 1. Chemical structure of BPDA-PDA PI and ODPA-3SDA PI.

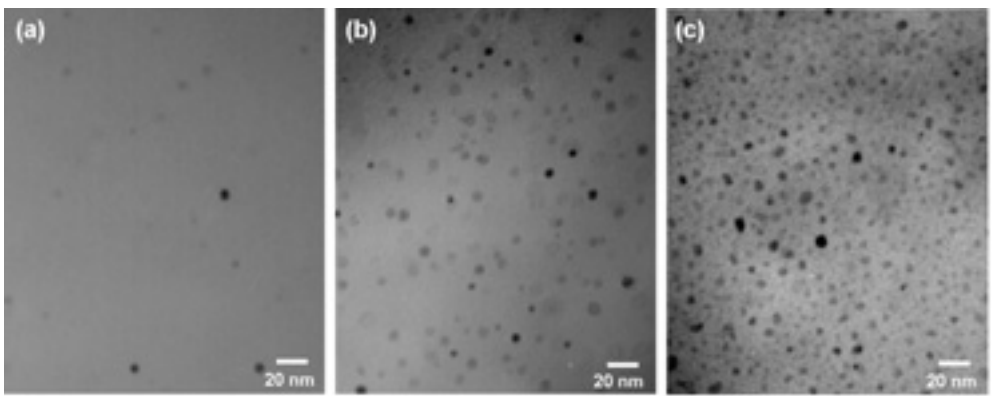

Figure 2. TEM plan-view images of ZnO nanoparticles in BPDA-PDA type PI films with different curing times in a nitrogen atmosphere: (a) which was cured at 350°C for 1 h; (b) cured at 350°C for 2 h; (c) cured at 350°C for 4 h.

at 350°C for 1 h, particles were rarely observed but particle size and density increased as curing time increased from 1 h. The nanoparticles cured at 350°C for 1, 2, and 4 h were about 4, 4.3, and 5.6 nm in diameter, respectively. Nanoparticles were formed in the PI with a very high density, seen in figure 2(c). Figure 3 shows the corresponding selected area electron diffraction patterns of figure 2. A pattern analysis indicated the particles were identified as zinc oxide with a hexagonal crystal structure in all specimens. The diffraction pattern became sharper with increasing curing time, which suggests that the density and size of the nanoparticles increased with curing time. Figures 4(a)–(c)

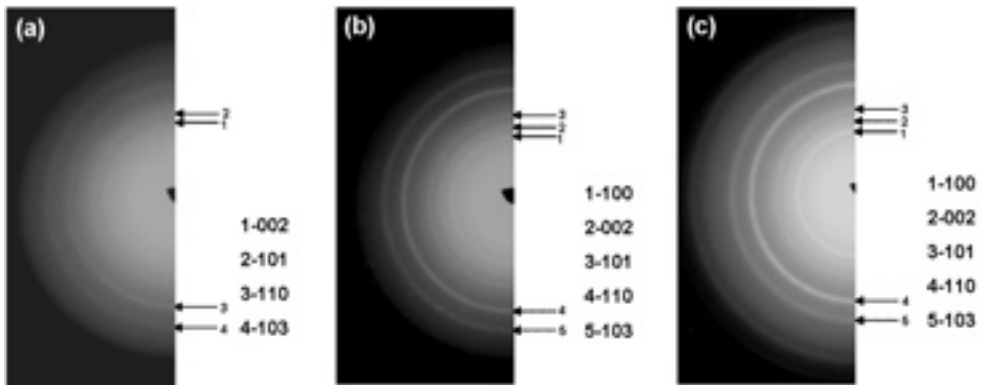

Figure 3. Selected area diffraction patterns of ZnO nanoparticles in BPDA-PDA type PI films with different curing times in a nitrogen atmosphere: (a) 350°C for 1 h; (b) 350°C for 2 h; (c) 350°C for 4 h.

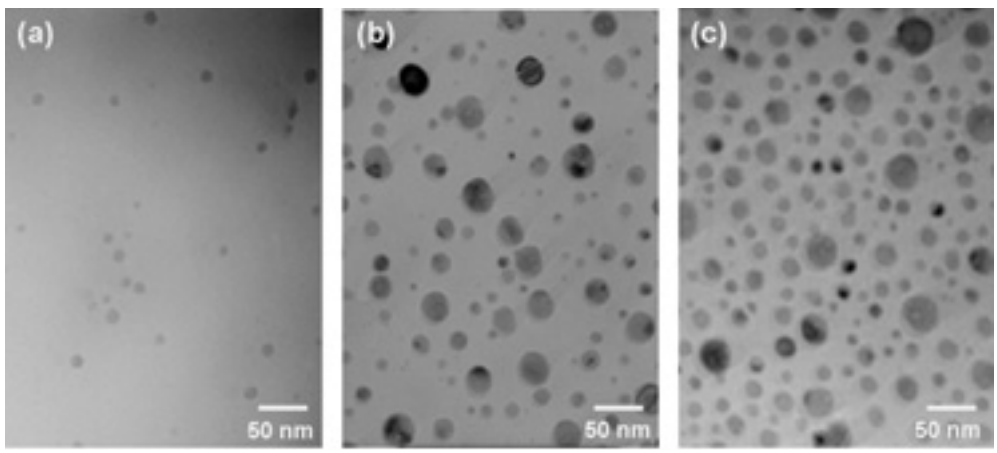

Figure 4. TEM plan-view images of ZnO nanoparticles in BPDA-PDA type PI films with different curing times in a vacuum atmosphere: (a) which was cured at 350°C for 1 h; (b) cured at 350°C for 2 h; (c) cured at 350°C for 4 h.

show the plane-view images of BPDA-PDA/Zn (10 nm) film cured at 350°C for 1, 2 and 4 h in a vacuum. The same trend was observed for the specimens cured in a nitrogen atmosphere (figure 2). Nanoparticles were hardly formed in PI after curing at 350°C for 1 h and the density of particles increased with curing time. However, in the specimens that were cured for 2 and 4 h, a bimodal distribution of particles was observed. The particle formation in a vacuum was different from that in a nitrogen atmosphere. The shape of large or small particles dispersed in PI thin film was also spherical. The average

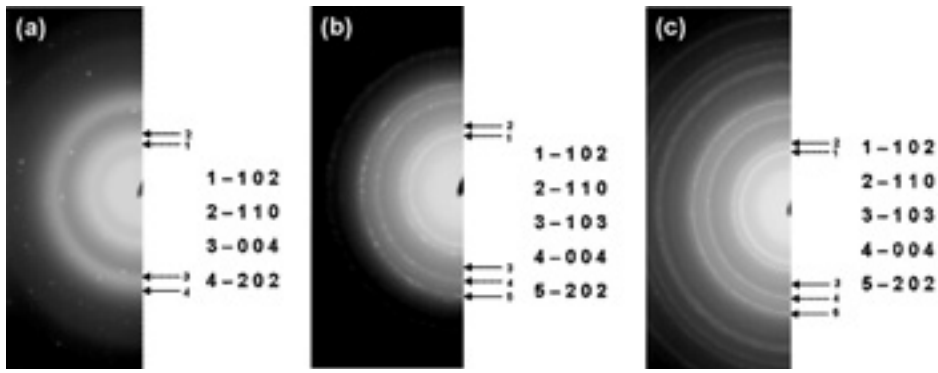

Figure 5. Selected area diffraction patterns of ZnO nanoparticles in BPDA-PDA type PI films with different curing times in a vacuum atmosphere: (a) 350°C for 1 h; (b) 350°C for 2 h; (c) 350°C for 4 h.

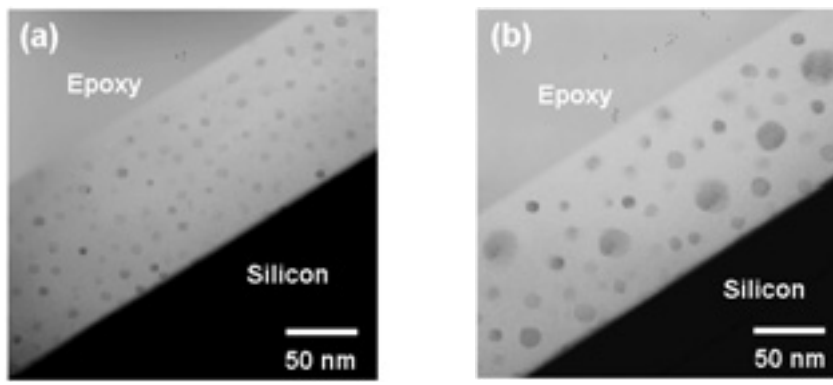

Figure 6. TEM cross-sectional images of ZnO nanoparticles in BPDA-PDA type PI films with cured at 350°C for 4 h: (a) nitrogen atmosphere; (b) vacuum atmosphere.

size of particles cured at 350°C for 1, 2, and 4 h was about 8.5 nm, about 14.2 nm, and about 17.7 nm in diameter, respectively. The average size of particles in the specimen cured in a vacuum was larger than that of specimens cured in N_2 at the same curing time. Nanoparticles formed in the PI layer were also confirmed to be zinc oxide by using the selected area diffraction pattern analysis as shown in figure 5. Ring patterns also became sharper with curing time, which is similar to the results obtained in N_2-cured specimens. Figure 6 shows the cross-sectional TEM images of BPDA-PDA/Zn film which were cured at 350°C for 4 h in a nitrogen atmosphere and in a vacuum. Zinc oxide nanoparticles were randomly distributed in the PI layer and unreacted Zn metal layers were not observed at the PI/Si interface in both cases. The observation shows the size and density of particles

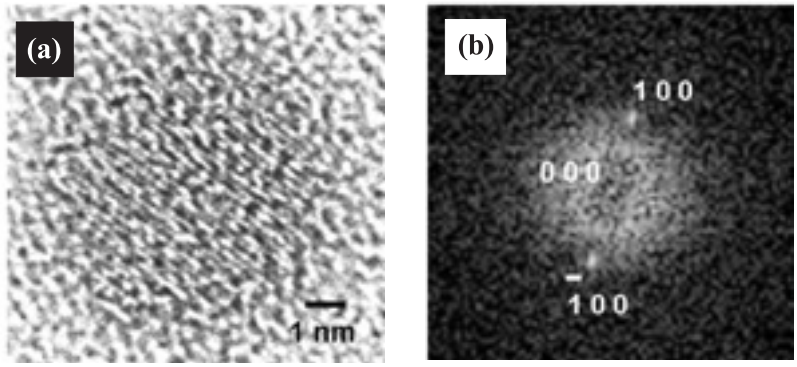

Figure 7. (a) High resolution TEM image and (b) Fourier transformation image of ZnO nanoparticles in BPDA-PDA type PI films with cured at 350°C for 4 h in a nitrogen atmosphere.

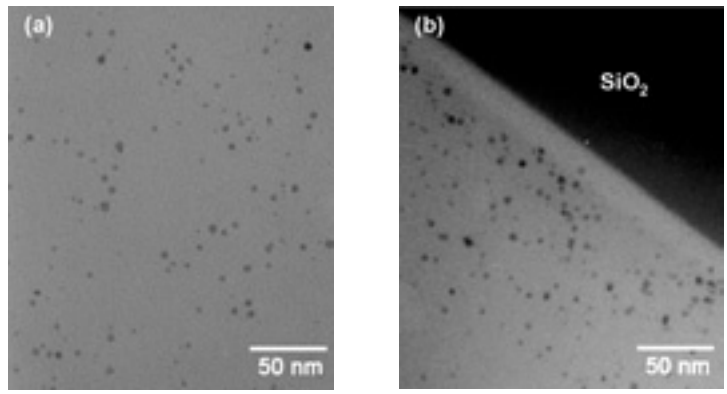

Figure 8. TEM images of Zn oxides in ODPA-3SDA type PI films with cured at 250°C for 1 h: (a) plane-view image. (b) cross-sectional image.

were similar to those of plane-view results (figures 2(c), 4(c)). Figure 7(a) is a high-resolution lattice image of the zinc oxide nanoparticles obtained in the specimen cured at 350°C for 4 h in a nitrogen atmosphere. Lattice fringes attest that the particles were well crystallized. A single pattern of lattice image in a single particle and the corresponding Fourier transformation results prove that the particle is indeed a single crystal containing no other secondary structures or grain boundaries. Many lattice images were observed and all of the particles were single crystals.

Figure 8 shows the TEM images of nanoparticles formed inside the ODPA-3SDA PI film by curing at 250°C for 1 h in a nitrogen atmosphere. It revealed that relatively small zinc oxide nanoparticles were formed and the average size of particles was about 4.8 nm.

The crystal structure of particles was also identified as hexagonal zinc oxide. In this case PI thickness after curing was comparatively thick, so particles in the ODPA-3SDA PI film were distributed nearly in the interface between PI and substrate.

4. DISCUSSION

The results showed that the size, distribution, and density of zinc oxide particles strongly depended on the curing time and curing atmosphere. Initially, the PAA, being a relatively strong acid, attacks the Zn layer, creating the PAA complexes [20]. It is clear that thin Zn metal that reacted with PAA was completely dissolved in the PI film because unreacted Zn metal layers were not observed in the interface between PI and substrate.

During imidization, the amic acid is depolymerized to diamines and dianhydrides. As the imidization process proceeds, it reforms amic acid linkage and then undergo imidization [22, 23]. Deprotonation of carboxylic acid is known to be an important step in thermal imidization, which means that residual solvent can catalyze the imidization reaction chemically as well as increasing the chain mobility [23]. During the imidization reaction, the Zn ions react with oxygen or water generated from the imidization process, and oxide particles precipitate as a by-product. The amount of particles formed is commensurate with the degree of imidization. When PAA/zinc thin films were cured at 350°C for 1 h, imidization may be incomplete and both PAA and zinc ions still exist in the polyimide film. Therefore, longer isothermal imidization time resulted in the formation of zinc oxide particles with a higher density. When the curing time increased, the coalescence of particles also occurred to reduce the surface energy. Mobility of zinc ions are generally enhanced by the presence of solvent, so they can disperse into PAA film, which makes the formation of uniform fine particles possible during the curing process [23]. The lattice images of zinc oxide particles showed that they are single crystals. These particles nucleated and grew. Although Ni particles formed from the reaction between PAA and NiFe thin films, some Ni particles were not single grains, which demonstrated that only a part of the NiFe film was attacked by PAA [18].

The zinc oxide particles formed during curing in a vacuum were noticeable. The water vapor which was produced from the imidization process (figure 1) reacted with Zn to form zinc oxide since oxygen from outside rarely diffused into the PI in a vacuum. The particle size and size distribution depended on the curing environment. The imidization degree was affected by the curing environment [20, 21]. The evaporation rate of solvent and the reaction by-product, water vapor can be changed with curing condition. These effects should influence the particle formation. Further systematic study is in progress.

As shown in figure 8, we also confirmed that zinc oxide nanoparticles formed the ODPA-3SDA type PI film during curing. Our mechanism of the formation of nanoparticles in BPDA-PDA type PI seems to have operated in this type of PI. PAA dissolved thin film metal and nanoparticles formed during imidization. The polyimide curing condition was sensitive to the PI type. The particle size and distribution could be controlled by changing curing time and temperature according to PI. Furthermore, the particle density

can be changed by changing the initial metal thickness [19]. Meanwhile, ODPA-3SDA type PI, which is colorless and has high optical transparency, can be of more practical use for optical applications [24].

5. CONCLUSION

In summary, single crystal zinc oxide nanoparticles dispersed in the PI layer were fabricated by imidization reaction between Zn metal film with PAA. TEM images and indexed diffraction patterns showed that zinc oxide nanoparticles formed regardless of the polyimide type and curing conditions. The individual nanoparticles have a single crystal structure as can be seen from figure 7. Both curing time and atmosphere have an influence on zinc oxide nanoparticle formation in PI film.

Acknowledgements. This research was supported by a grant (code #: 05K1501-02510) from 'Center for Nanostructured Materials Technology' under '21st Century Frontier R&D Programs' of the Ministry of Science and Technology, Korea. The authors would also like to thank Dr. Jong Chan Won from Korea Research Institute of Chemical Technology (KRICT) for his generous supply of polyimide materials.

NOTE

1. Author to whom correspondence should be addressed: e-mail: kimyh@hanyang.ac.kr

REFERENCES

[1] Wilson A M and Mittal K L ed. 1984 *Polyimides: Synthesis, Characterization, and Applications* (New York: Plenum Press)

[2] Feger C, Doane D A and Franzon P D ed. 1993 *Multichip Module Technologies and Alternatives* (New York: Van Nostrand Reinhold)

[3] Ree M, Shin T J and Lee S W 2001 *Korea Polymer J.* **9** 1

[4] Ree M 2006 *Macromol. Res.* **14** 1

[5] Alivisatos A P 1996 *Science* **271** 933

[6] Schmid G 2004 *Nanoparticles: From Theory to Application* (Weinheim: Wiley-VC)

[7] Baraton M I 2003 *Synthesis, Functionalization and Surface Treatment of Nanoparticles* (USA: American Scientific Publishers)

[8] Bae D-S, Kim E-J, Bang J-H, Kim S-W, Han K-S, Lee J-K, Kim B-I and Adair J H 2005 *Metals Mater. Int.* **11** 291

[9] Fukumi K, Chayahara A, Kadono K, Sakaguchi T, Horino Y, Miya M, Fujii K, Hayakawa J and Satou M 1994 *J. Appl. Phys.* **75** 3075

[10] Mahamuni S, Bendre B S, Leppert V J, Smith C A, Cooke D, Risbud S H and Lee H W H 1996 *Nanostructured Mater.* **7** 659

[11] Salata O V, Dobson P J, Hull P J and Hutchison J L 1994 *Thin Solid Films* **251** 1

[12] Mahamuni S, Borgonhain K and Bendre B S 1999 *J. Appl. Phys.* **85** 2861

[13] Kowalczyk S P, Kim Y-H, Walker G F and Kim J 1988 *Appl. Phys. Lett.* **52** 375

[14] Kim Y-H, Walker G F, Kim J and Park J 1987 *J. Adhesion Sci. Tech.* **1** 331

[15] Chung Y, Park H P, Jeon H J, Yoon C S, Lim S K and Kim Y-H 2003 *J. Vac. Sci. Tech*. **21** L9
[16] Lim S K, Chung K J, Kim Y-H, Kim C K and Yoon C S 2004 *J. Magn. and Magn. Mat*. **272–276** Supplement 1 E1167
[17] Lim S K, Yoon C S, Kim C K and Kim Y-H 2004 *J. Phys. Chem*. **108** 18179
[18] Lim S K, Chun I S, Ban K S, Yoon C S, Kim C K and Kim Y-H 2006 *J. Colloid Interface Sci.* **295** 108
[19] Park H P, Chung Y, Yoon C S, Jo S S and Kim Y-H 2004 *Mater. Sci. Forum* **449–452** 1237
[20] Jeon H J, Chung Y, Kim S Y, Yoon C S and Kim Y-H 2004 *Mater. Sci. Forum* **449–452** 1145
[21] Song M S, Yoon C S and Kim Y-H 2005 *Mater. Sci. Forum* **475–479** 3555
[22] Brekner M J and Feger C 1987 *J. Polym. Sci, Polym. Chem*. **25** 2005
[23] Mittal K L 1989 *Polyimides: Synthesis, Characterization, and Applications* (New York: Plenum)
[24] Li X-D, Zhong Z-X, Han S-H, Lee S H and Lee M-H 2005 *Polym. Int*. **54** 406